

AIS-2 SPECTRA OF CALIFORNIA WETLAND VEGETATION

MICHAEL F. GROSS, College of Marine Studies, University of Delaware, Newark, DE 19716, USA; SUSAN L. USTIN, Department of Botany, University of California, Davis, CA 95616, and Space Sciences Laboratory, University of California, Berkeley, CA 94720, USA; VYTAUTAS KLEMAS, College of Marine Studies, University of Delaware, Newark, DE 19716, USA.

ABSTRACT

Spectral data gathered by AIS-2 from wetlands in the San Francisco and Suisun Bays, California, on 11 September 1986 were analyzed. Spectra representing stands of green Salicornia virginica, green Sesuvium verrucosum, senescing Distichlis spicata, a mixture of senescing Scirpus acutus and Scirpus californicus, senescing Scirpus paludosus, senescent S. paludosus, mowed senescent S. paludosus, and soil were isolated. No difference among narrow-band spectral reflectance of the cover types was apparent between 0.8-1.6 μ m. There were, however, broad-band differences in brightness. These differences were sufficient to permit a fairly accurate decomposition of the image into its major cover type components using a procedure that assumes an additive linear mixture of surface spectra.

INTRODUCTION

The primary objective of our study is to compare AIS spectra of various wetland vegetation types. Ultimately, we hope to use imaging spectrometer data to identify vegetation types and their status (e.g. green, senescing, stressed). Gross and Klemas (1985, 1986) reported differences in the AIS-1 spectral response of Delaware wetland vegetation types, enabling them to be distinguished. Most of the spectral differences occurred between 1.4-1.9 μ m, and may have been influenced by second order overlap (Vane 1986). To continue these investigations, we analyzed AIS-2 data collected over intertidal wetlands in the Suisun and San Francisco Bays of California. The vegetation in the California marshes exhibited greater spatial and community heterogeneity than that in the Delaware marshes.

DATA ACQUISITION AND ANALYSIS

Three flightlines of AIS-2 data were acquired in Tree Mode (0.8-2.2 μ m, with the useful region [i.e. no second order overlap effects] approximately 0.8-1.6 μ m) on 11 September 1986 at about 21:00 GMT: one over salt marshes in the southern part of San Francisco Bay, and two covering the brackish Suisun Marsh in Suisun Bay. Within a few days preceding and following the date of flight, spectra of various wetland soils and of green, senescing, and senescent (dead) wetland vegetation species were obtained from field samples using a VIRIS (Visible/Infrared Intelligent Spectroradiometer). One to four samples of each cover type were obtained. In addition, accessible regions of the marsh were visited by car and on foot, permitting mapping of the various cover types and observations of site characteristics. Four days after the flight, photo-

graphs of the flightline areas were taken from a low-altitude aircraft and used to identify surface cover.

The AIS data were analyzed at the Space Sciences Laboratory of the University of California (Berkeley) using SPAM (Spectral Analysis Manager) software developed by the Jet Propulsion Laboratory. No radiometric calibration had been applied to the data by JPL. Observation of the raw data revealed substantial vertical striping and geometric distortions resulting from aircraft movements. Horizontal striping was not evident. We chose to analyze a portion of the flightline encompassing parts of Joice and Grizzly Islands in the Suisun Marsh (Fig. 1). This area was selected because it had been extensively groundtruthed and contained the majority of marsh cover types. The leveed wetlands in the study region are managed to optimize waterfowl habitat, such that tidal flooding and salinity are controlled, thus causing vegetation distribution and condition to differ between ponds. At the time of AIS data collection, dry summer weather and lack of tidal flooding had resulted in the senescence of much of the marsh vegetation.

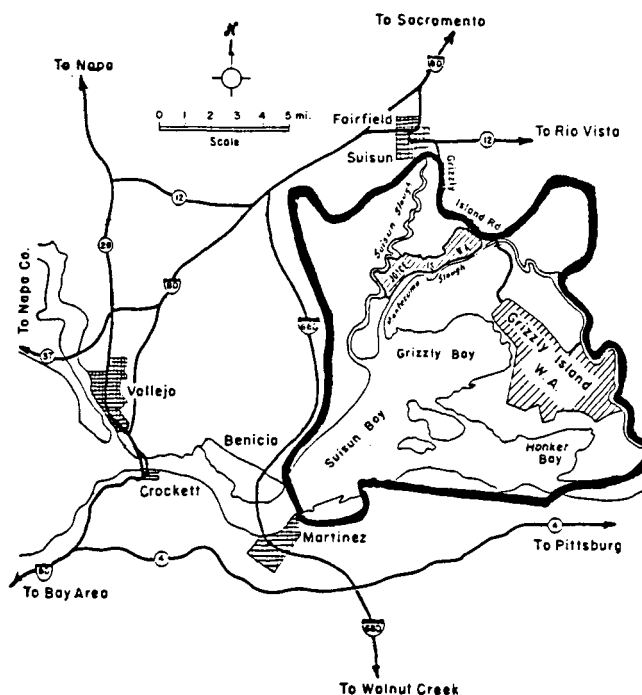


Fig. 1. Location of Suisun Marsh (area within thick solid line).

The area of interest was divided into two 512-line segments and one 400-line segment for analysis. One of the 512-line segments was free of large water bodies, but the other two contained significant portions of large, vertically oriented sloughs filled with water. Analysis of the raw data demonstrated that the vertical striping was too severe to permit a meaningful extraction of information. To destripe the image, a program that computes the mean data value for an entire scene in each spectral band and then adjusts the column mean in each band to match the corresponding scene mean value was employed. This program assumes that, over the entire length of the image segment, the mean brightness value is the

ORIGINAL PAGE IS
OF POOR QUALITY

same for each of the 64 columns of data. This technique was effective only on the segment free of major vertical water features; we thus chose to concentrate our analysis on this part of the data. Wavebands beyond $1.58\mu\text{m}$ (bands 73-128) were avoided to minimize second order overlap effects.

RESULTS

Destriping the AIS data resulted in a significant improvement in the visual appearance of the data (Figs. 2 and 3) and in a substantial reduction in the noise of plotted spectra. To derive spectra of various cover types in the image, the mean spectrum of 2×2 to 5×5 pixel samples ($n = 3-14$) of distinct vegetation types or soil was computed and considered to represent the spectral response of the cover type. The eight distinct cover types identified were green Salicornia virginica (pickleweed), green Sesuvium verrucosum (purslane), senescing Distichlis spicata (salt-grass), senescing Scirpus acutus and Scirpus californicus (tules), senescing Scirpus paludosus (alkali bulrush), senescent S. paludosus, mowed senescent S. paludosus, and dry soil. A mean spectrum for the entire image was then approximated by computing the mean spectrum of seven evenly-spaced 10×64 segments from the image. These nine spectra were stored in a library.

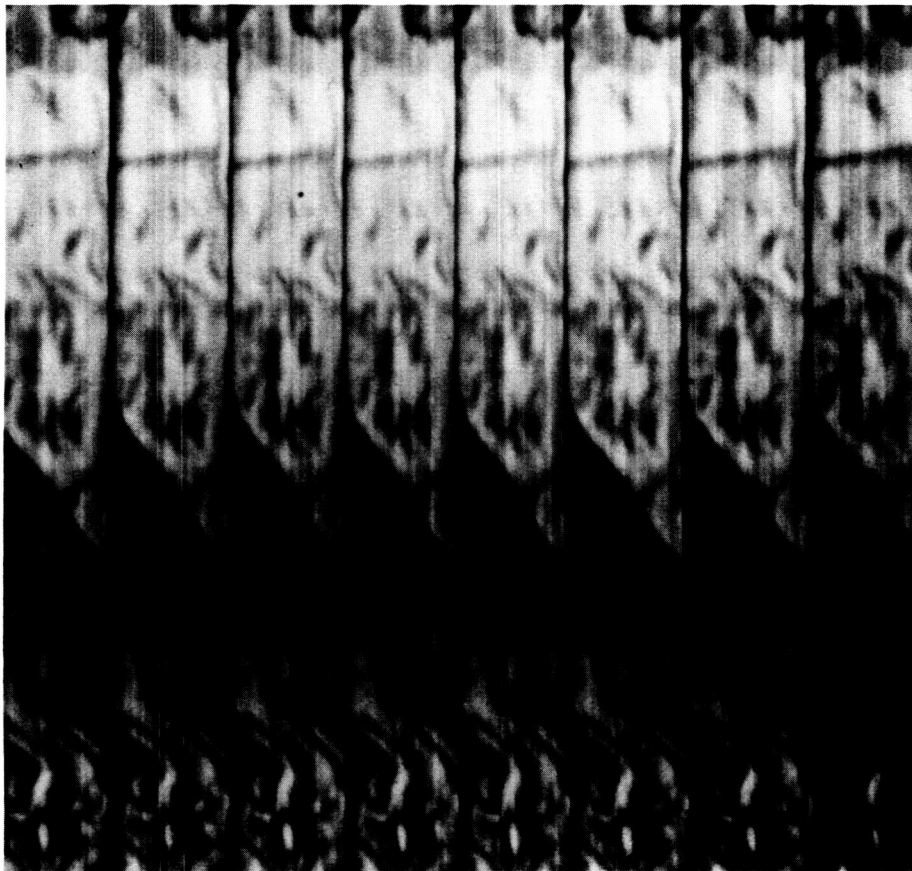


Fig. 2. Raw AIS-2 data, $1.27-1.35\mu\text{m}$.

ORIGINAL PAGE IS
OF POOR QUALITY.

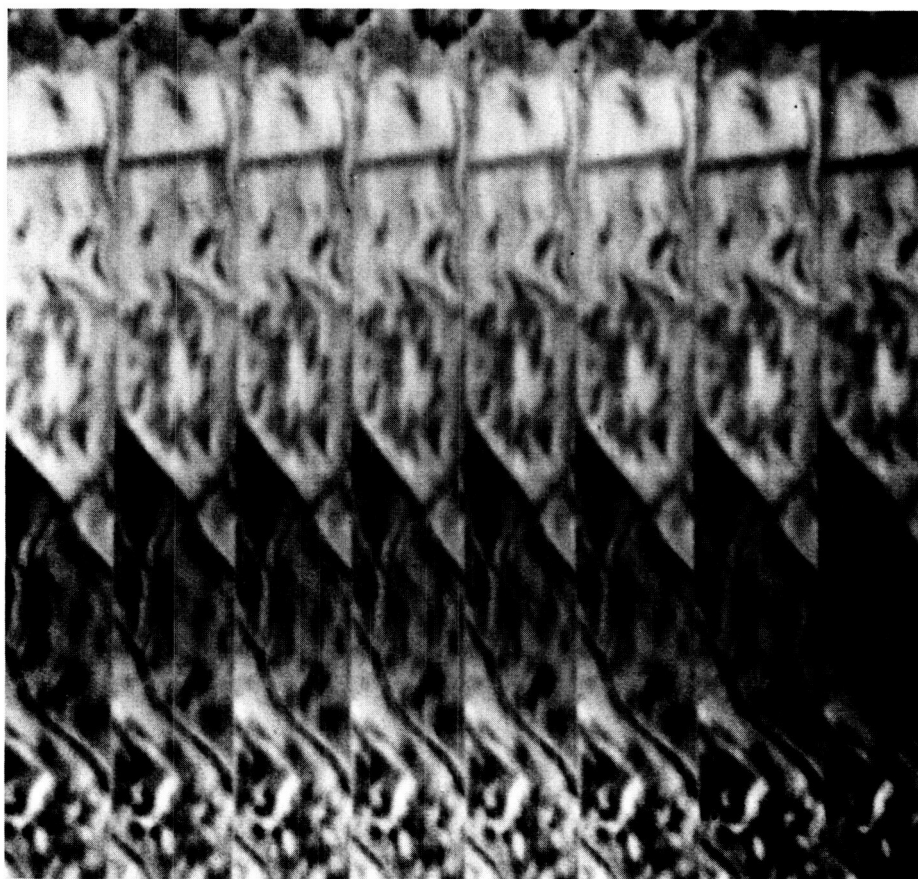


Fig. 3. Vertically destriped AIS-2 data, 1.27-1.35 μ m.

Spectra were displayed in both normalization modes (area and amplitude). Spectra were compared within four groups of wavebands separated by atmospheric absorption features: 0.80-97 μ m, 0.97-1.15 μ m, 1.15-1.44 μ m, and 1.44-1.58 μ m (Table 1). Figure 4 shows spectra from the cover types between 1.15-1.44 μ m, displayed in amplitude normalization mode. No narrow spectral band reflectance features were evident within any waveband segment; only broad-band differences in brightness were apparent.

The VIRIS data were also displayed in normalized amplitude mode, and the spectra were visually compared amongst themselves and with AIS spectra. Similar cover types exhibited generally similar VIRIS spectra. There were some broad-band differences in brightness between species, and may have been some narrow-band differences. However, the number of replicates ($n = 1-5$) was too small, the field of view of the instrument ($\approx 1\text{cm}^2$) insufficient, and the level of noise (resulting from wind, variable irradiance conditions, and the instrument) too high, to ascertain whether such narrow-band differences were real.

To determine whether the observed AIS brightness differences were sufficient to permit discrimination of cover types, we ran the CLUSTER (unsupervised classification) program, with and without the "manual" option, several times using different noise and cluster thresholds. Although the algorithm did create several classes, their distribution

did not correspond closely to that of the cover types and appeared to be largely random. In addition, some classes were composed of vertical stripes resulting from unequal detector response.

Table 1. Relative brightness of eight wetland cover types, displayed in amplitude normalization and area normalization modes.

Cover Type	Display Mode	.80-.97 μ m	.97-1.15 μ m	1.15-1.44 μ m	1.44-1.58 μ m
Green					
<u>Salicornia virginica</u>	Amp.	<	<	<	=
	Area	=	<,>*	=	=
Green					
<u>Sesuvium verrucosum</u>	Amp.	<	<	<	=
	Area	=	=	=	=
Senescing					
<u>Distichlis spicata</u>	Amp.	=	=	=	=
	Area	=	=	=	=
Senescing					
<u>Scirpus acutus</u> and	Amp.	=	=	=	=
<u>Scirpus californicus</u>	Area	=	=	=	=
Senescing					
<u>Scirpus paludosus</u>	Amp.	=	=	=	=
	Area	=	=	=	=
Senescent					
<u>S. paludosus</u>	Amp.	=	=	=	=
	Area	=	=	=	=
Mowed					
Senescent	Amp.	>	>	>	=
<u>S. paludosus</u>	Area	=	=	=	=
Dry Soil	Amp.	=	=	=	=
	Area	=	=	=	=

*S. virginica had the lowest radiance between 0.98-1.04 μ m, but the highest radiance between 1.05-1.11 μ m. Relative brightness between cover types should be compared for similar display modes within a column. For example, between 1.15-1.44 μ m in amplitude normalization mode, mowed senescent S. paludosus was the brightest, S. virginica and S. verrucosum the darkest, and the other five spectra were intermediate and similar in brightness.

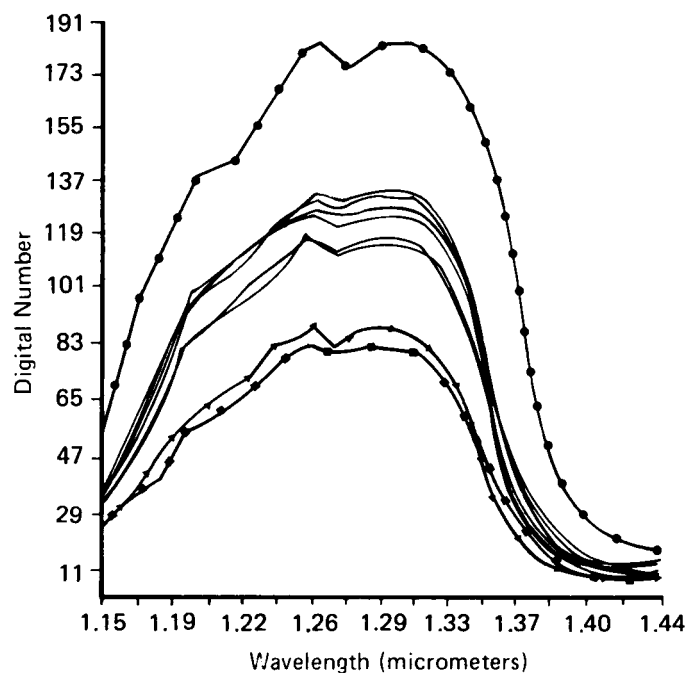


Fig. 4. Mean scene spectrum and spectra of eight cover types, shown between 1.15-1.44 μ m in amplitude normalization mode.
 -●-●-●- = mowed senescent *S. paludosus*, -▲-▲-▲- = *S. verrucosum*,
 -■-■-■- = *S. virginica*. The other six spectra are clustered between the first three spectra.

Better results were achieved with MIXTURE, a program that, when used in the area mode, assigns pixels to classes based on user-specified spectra (somewhat analogous to a supervised classification). The distribution of cover types assigned by the algorithm corresponded well to the actual distribution when spectra of only three cover types (green *Salicornia*, senescing *D. spicata*, and mowed dead *S. paludosus*) were specified (Fig. 5), as well as when all eight cover type spectra were specified. The relatively featureless residual image (column 5 in Fig. 5) supports the interpretation that the user-defined spectra encompassed most of the spectral variation within the image. When used in plot mode, MIXTURE breaks a selected segment of the scene into its surface components, by percent, based on user-defined component spectra. Use of this program yielded good correspondence with ground data when used on areas composed of only two dominant cover types (green *S. virginica* and senescent *S. paludosus*), but poor results on more complex parts of the image. The two vegetation types represent some of the greatest spectral divergence of those measured and suggest that the spectral mixing was

responding to changes in moisture content or to the architecture-related shadowing of the canopies.

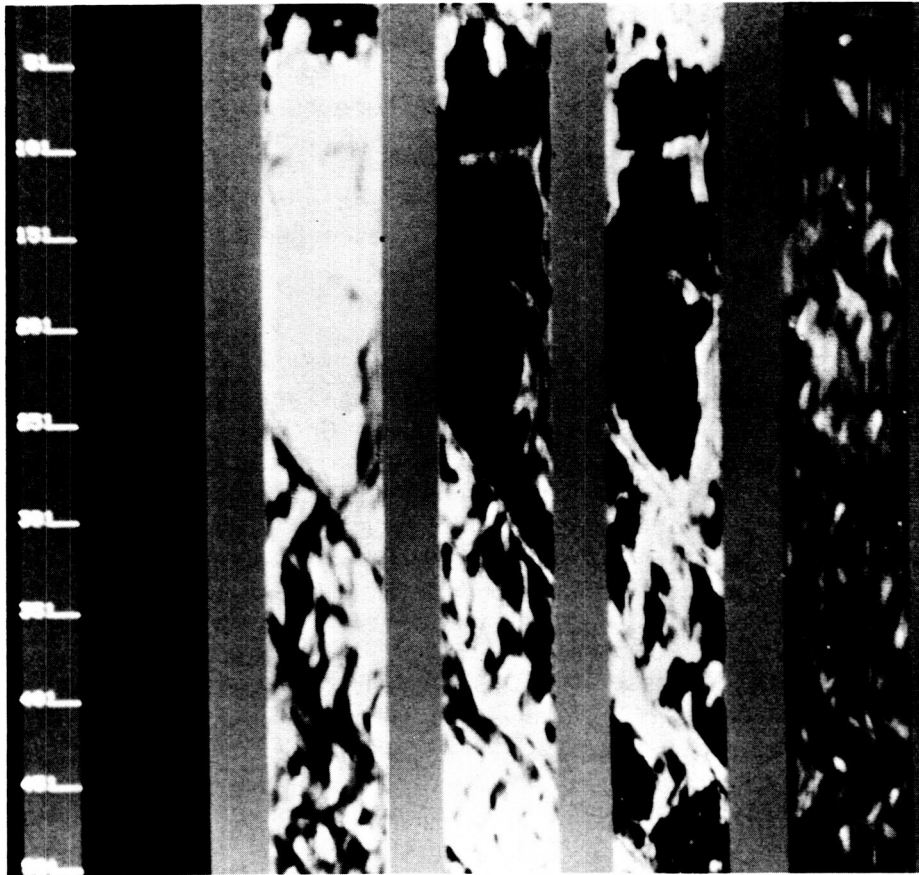


Fig. 5. Results of MIXTURE analysis, using three spectra (mowed dead *S. paludosus* [column 2], green *S. virginica* [column 3], senescing *D. spicata* [column 4]). Column 1 is blank, and column 5 is the residual, or pixels whose spectra do not match any of the three spectra.

DISCUSSION

No distinguishing narrow-band absorption or reflectance features were apparent among the soil or vegetation types at the wavelengths studied. In particular, we examined senescent vegetation spectra for evidence of cellulose features, but could identify only those also present in soil and succulent green vegetation spectra. Examination of the ground-gathered spectroradiometric measurements collected for this study revealed similar results. The only differences in AIS spectra were broad-band brightness differences, i.e. differences in radiance of particular cover types within broad wavebands. Despite the lack of distinct narrow-band spectral differences in cover types, it is encouraging that the broad-band brightness differences alone were sufficiently consistent to permit discrimination of various vegetation types. It is unfortunate that the data acquired beyond $1.6\mu\text{m}$ could not be used, since there is some evidence

that distinct spectral signature features may exist between 1.6 and 1.9 μ m (Gross and Klemas 1985, 1986; Spanner and Peterson 1986, Ustin et al. 1986, Wood and Beck 1986).

Our results suggest that, for vegetation studies, more consideration should be given to analysis techniques designed to maximize the extraction of the information contained in broad-band brightness differences. Given the apparent similarity in the shape of infrared spectra of various vegetation types, broad-band brightness differences apparently related to canopy moisture and/or architectural geometry may be the most important factor in vegetation studies using infrared data. We anxiously await AVIRIS data, which will be better calibrated and include information in narrow-band visible wavelengths that are expected to be more useful for vegetation analyses.

ACKNOWLEDGEMENTS

This research was supported by the NASA Earth Science and Applications Division Land Processes Program under Grant No. NAGW-950, and the Universities of Delaware and California. The authors wish to thank Paul Ritter at UC-Berkeley for assistance in analyzing the AIS data, Gordon Hoover of JPL for collecting and analyzing the VIRIS data, and Heather Froozandeh for secretarial expertise.

LITERATURE CITED

- Gross, M.F. and V. Klemas. 1985. Discrimination of coastal vegetation and biomass using AIS data. Pp. 129-133 in Proc. AIS Data Anal. Wkshop., Jet Propulsion Lab., Pasadena, CA. JPL Publ. 85-41.
- Gross, M.F. and V. Klemas. 1986. The use of Airborne Imaging Spectrometer (AIS) data to differentiate marsh vegetation. Remote Sens. Environ. 19(1):97-103.
- Spanner, M.A. and D.L. Peterson. 1986. Analysis of AIS data of the Bonanza Creek Experimental Forest, Alaska. Pp. 144-152 in Proc. Second AIS Data Anal. Wkshop., Jet Propulsion Lab., Pasadena, CA. JPL Publ. 86-35.
- Ustin, S.L., B.N. Rock and R.A. Woodward. 1986. Patterns of vegetation in the Owens Valley, California. Pp. 180-186 in Proc. Second AIS Data Anal. Wkshop., Jet Propulsion Lab., Pasadena, CA. JPL Publ. 86-35.
- Wood, B.L. and L.M. Beck. 1986. Trace element-induced stress in freshwater wetland vegetation: Preliminary results. Pp. 171-179 in Proc. Second AIS Data Anal. Wkshop., Jet Propulsion Lab., Pasadena, CA. JPL Publ. 86-35.
- Vane, G. 1986. Introduction. Pp. 1-16 in Proc. Second AIS Data Anal. Wkshop., Jet Propulsion Lab., Pasadena, CA. JPL Pub. 86-35.